Current Applied Physics 20 (2020) 1441–1446

Contents lists available at ScienceDirect

Current Applied Physics

journal homepage: www.elsevier.com/locate/cap

Optimized annealing conditions to enhance stability of polarization in sputtered $HfZrO_x$ layers for non-volatile memory applications

Yeriaron Kim [a,b], Jiyong Woo [e], Solyee Im [a], Yeseul Lee [c], Jeong Hun Kim [a], Jong-Pil Im [a], Dongwoo Suh [a], Sang Mo Yang [d], Sung-Min Yoon [b,*], Seung Eon Moon [a,**]

[a] ICT Creative Research Laboratory, Electronics and Telecommunications Research Institute, Daejeon, 34129, South Korea
[b] Department of Advanced Materials Engineering for Information and Electronics, Kyung Hee University, Yongin, Gyeonggi, 17104, South Korea
[c] Department of Physics, Sookmyung Women's University, Seoul, 04310, South Korea
[d] Department of Physics, Sogang University, Seoul, 04107, South Korea
[e] School of Electronics Engineering, Kyungpook National University, Daegu, 41566, South Korea

A R T I C L E I N F O

Keywords:
$HfZrO_2$
Ferroelectricity
Sputtering
Annealing

A B S T R A C T

In this paper, we report stable polarization switching in metal-$HfZrO_x$ (HZO)-metal capacitors when pulses are repeatedly applied from the initial state. By examining various process parameters including annealing method, annealing temperature, and annealing time, we investigated the optimal conditions for realizing ferroelectricity in HZO layers deposited by sputtering systems. More specifically, we examined how polarization behaviors evolved as a function of annealing temperatures. Our results showed that annealing HZO capped by a top electrode, when annealing temperature was higher than 850 °C, drives the transformation to large quantities of orthorhombic phases, and enables constant remnant polarization without the fluctuations caused by wake-up and fatigue. We continued to observe stable polarization up to 10^8 cycles with a pulse width of 5 μs.

1. Introduction

Hafnium oxide (HfO_2) based ferroelectric devices have recently attracted considerable attention. These binary oxide materials, which are frequently used for gate dielectrics in state-of-the-art transistors, are being further explored for versatile applications such as non-volatile memories [1–3]. Until now, ferroelectricity has been considered to result from a structural transformation into a certain metastable crystalline phase known as the orthorhombic phase [4,5]. Ever since ferroelectricity was first demonstrated in thin doped HfO_2 film [6], the effects of various dopants such as Si, Al, Y, and Zr have been experimentally explored to determine how the dopants affect the microstructures of the HfO_2 [7–10]. Additional annealing at high temperatures is known to promote thermodynamic phase transitions, and the incorporated dopants can stabilize the modified structure [11]. These conditions produce dipoles in the ferroelectric HfO_2 layers which can be spontaneously aligned, and even after voltage has been removed, show a remnant polarization (P_r).

From the device operation perspective, the P_r steadily increases in the pristine state with the application of electrical pulses [12–14]. It has been reported that electrical stress redistributes the defects that pin the dipoles, or further activates the phase transition to the orthorhombic phase [15,16]. This wake-up process allows more ferroelectric phases to be involved in the switching, resulting in the larger P_r. However, when the P_r reaches its maximum value it then begins to decrease due to fatigue or degradation resulting from charge trapping and domain pinning [17]. Since the ferroelectric HfO_2 layer is employed as a gate oxide in field effect transistors for memory applications [18–22], the instability of P_r during continuous field cycling results in a large variation in switching parameters, such as the number of charges induced at the channel.

To date, studies related to this stability have been conducted primarily on doped HfO_2 layers grown by atomic layer deposition [12–15, 23–27]. In practice, the HfO_2 layer can be also fabricated by sputtering systems [11,28–34], which saves deposition time and can be thus a more cost-effective process. Polarization switching has been demonstrated in sputtered ferroelectric HfO_2, taking into account the electrode materials and oxygen content during the sputtering process [29,32], but the stability of the P_r has rarely been discussed.

Therefore, the aim of this study is to identify optimized annealing

* Corresponding author.
** Corresponding author.
E-mail addresses: sungmin@khu.ac.kr (S.-M. Yoon), semoon@etri.re.kr (S.E. Moon).

https://doi.org/10.1016/j.cap.2020.09.013
Received 9 June 2020; Received in revised form 9 September 2020; Accepted 27 September 2020
Available online 9 October 2020

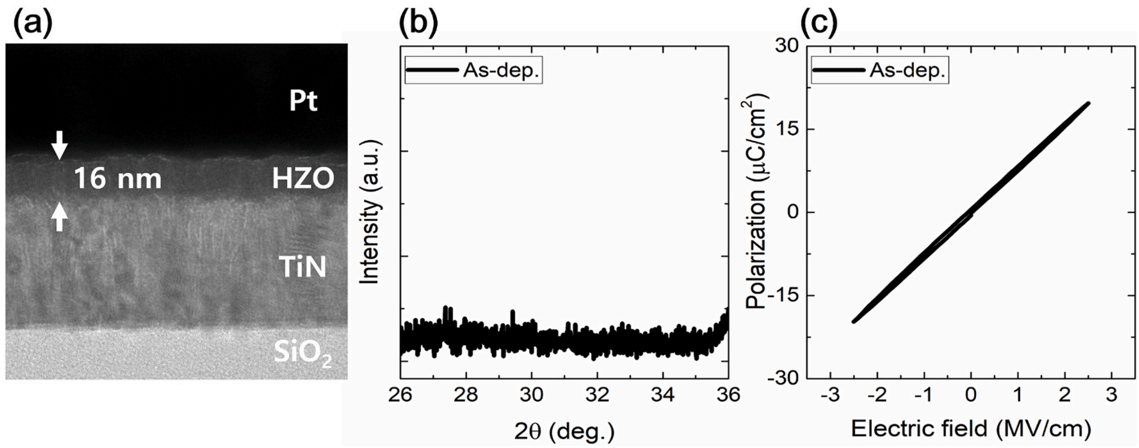

Fig. 1. (a) The TEM image of the Pt/HZO/TiN capacitor. (b) GIXRD peak for the as-deposited HZO film on the TiN bottom electrode. (c) The P-E curve of the Pt/HZO/TiN capacitor.

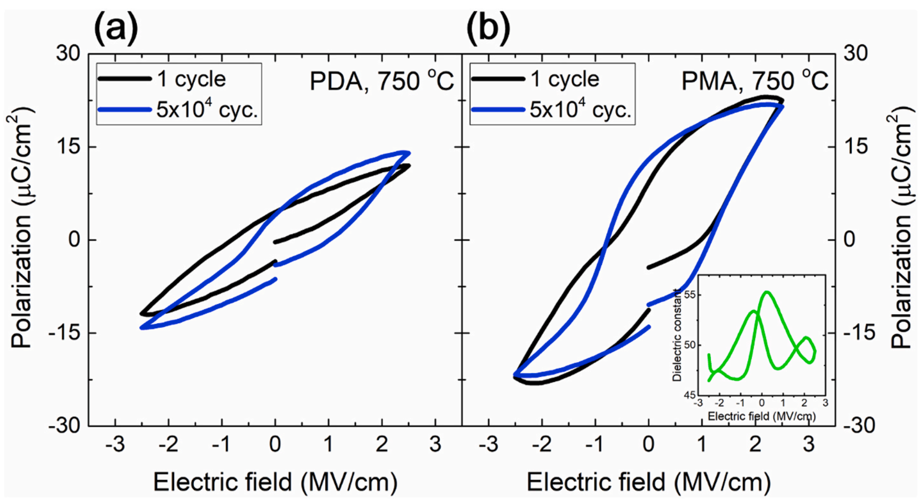

Fig. 2. The transition of P-E curves after 5×10^4 cycles of ±4 V with a pulse width of 50 μs for the capacitors annealed by the (a) PDA and (b) PMA at 750 °C. The antiferroelectric-like behavior from the C-E curve was shown in the inset of Fig. 2(b).

conditions that will ensure stable ferroelectric switching characteristics in the sputtered HfO_2 layer. We specifically show the impact of annealing parameters on polarization under repeated pulse cycling.

1.1. Experiment section

A 50-nm-thick TiN film as a bottom electrode (BE) was deposited on wet-oxidized Si wafer using sputtering. A 16-nm-thick $HfZrO_x$ (HZO) film was sputtered using a stoichiometric $Hf_{0.5}Zr_{0.=5}O_2$ compound target with an Ar plasma on top of the TiN BE at room temperature. 50-nm-thick Pt film was used for a top electrode (TE), resulting in a Pt TE/HZO/TiN BE capacitor structure. The capacitors can be annealed in two potential ways to realize ferroelectricity, so that post-deposition annealing (PDA) and post-metallization annealing (PMA) [35] were performed before and after the TE deposition, respectively. Hysteresis loops and fatigue stresses were evaluated using 1 kHz triangular pulses and 50 μs rectangular pulses with Precision LC II (Radiant) and TF analyzer 2000 (aixACT), respectively. Small-signal capacitance was measured using an Agilent 4285 A and Keithley-4200 with an AC probing signal of 20 mV. I–V characteristics also measured using Keithley-4200. To analyze crystal structure of HZO thin films, grazing-angle incidence X-ray diffraction (GIXRD) measurement was performed using D/MAX-2500 (RIGAKU) with Cu K alpha Source . The angle of incidence was 2°. For transmission electron microscopy (TEM) analysis to confirm the stacking of films on Si substrate, we prepared the sample by focused ion beam. To confirm the thickness of the HZO layer, a low-resolution (× 100 k) image was utilized using Talos F200X (FEI) tool.

2. Results and discussion

Fig. 1a shows a transmission electron microscopic (TEM) image of the fabricated Pt/HZO/TiN capacitor. The thickness of the deposited HZO layer was estimated to be about 16 nm. In the HZO before performing annealing, no noticeable peak intensity was observed in the entire range of 2θ between 26 and 36 through GIXRD analysis, as shown in Fig. 1b. Since the phases in the HZO layer were not yet crystallized into the particular phase, the capacitor exhibited a linear polarization response without hysteresis as a function of the electric field, as shown in Fig. 1c.

At a given annealing temperature of 750 °C, the PDA treated HZO layer initially showed a convex polarization shape with very small 2 remnant polarization (P_r) of about 7 μC/cm^2 measured at 0 MV/cm in the polarization-electric field (P-E) curve, as shown in Fig. 2a. As 5×10^4 pulses were repeatedly addressed to the capacitor, a somewhat sharp transition in the polarization was observed at positive and negative coercive fields (E_c), which can be defined by the field at zero polarization. On the other hand, a pinched hysteresis, where the slope of the

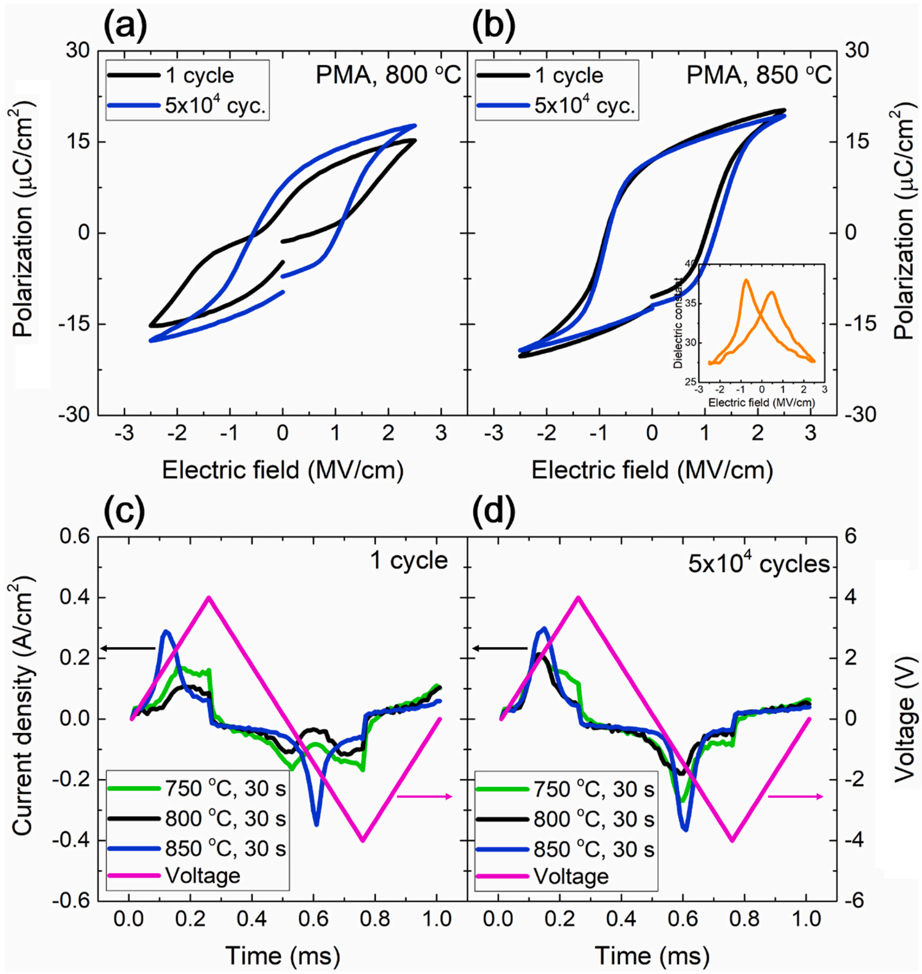

Fig. 3. The transition of P-E curves after 5×10^4 cycles of ±4 V with a pulse width of 50 μs for the capacitors annealed at (a) 800 and (b) 850 °C. The ferroelectric behavior from the C-E curve was shown in the inset of Fig. 3(b). Corresponding transient current density measured at the pristine state was shown in Fig. 3(c). (d) The behaviors of the current densities were changed by the pulses in most cases except the capacitor annealed at 850 °C.

polarization changed twice, was shown in the first cycle of the HZO annealed by PMA, as shown in Fig. 2b. Multiple peaks at relative dielectric constant were subsequently observed from the capacitance-voltage (C–V) measurements, as shown in the inset of Fig. 2b. However, consecutive pulses led to a ferroelectric P-E curve with 2 P_r of 30 μC/cm^2. These results imply that the orthorhombic phases with dipoles were formed more effectively when annealing HZO capped by TE [36,37]. However, the orientations of adjacent dipoles were opposite to each other in the pristine state, or the ferroelectric phases were disabled due to defects, resulting in an antiferroelectric-like P-E curve [22,23]. In this case, repeated electrical pulses that cause mechanical stress, known as a wake-up process, helped to align the dipoles with the field, or eliminate defects far from the ferroelectric phases [28]. This eventually promotes additional phase transition, allowing more activated phases to participate in the switching.

We then adjusted the annealing temperature during the PMA process. A similar transition from antiferroelectric-like pinched hysteresis to ferroelectric hysteresis was observed in the P-E trace when the annealing temperature was increased to 800 °C, as shown in Fig. 3a. Compared to the capacitor annealed at 750 °C, the absolute 2 P_r value was slightly lower, but the polarization changed rapidly and became saturated at E_c and high field, respectively. It has generally been reported that the polarization under high field is induced not only by spontaneous dipole moments but also by leakage components. When the field was swept up to 2.5 MV/cm, the interference from the leakage current became noticeable, resulting in a leaky hysteresis loop (Fig. 2b). In this regard,

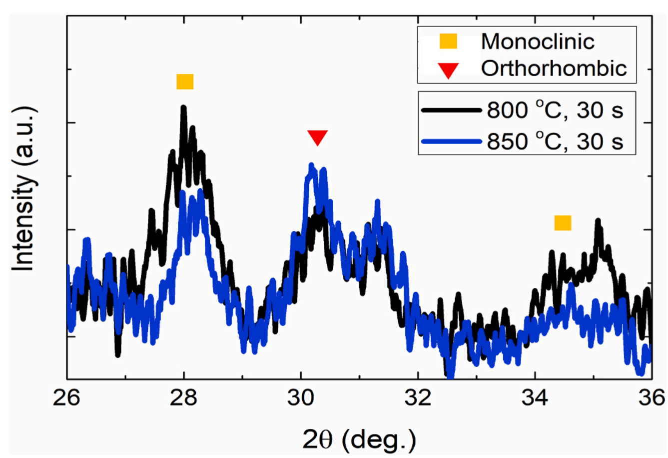

Fig. 4. The result of the GIXRD measurement of the HZO films annealed at 800 and 850 °C.

the higher annealing temperature enhanced polarization switching by preventing the unwanted leakage. Note that the ferroelectric property even began to be observed in the pristine state of the HZO when the annealing temperature was further increased to 850 °C, as shown in Fig. 3b. This result was in good agreement with the butterfly curve of the

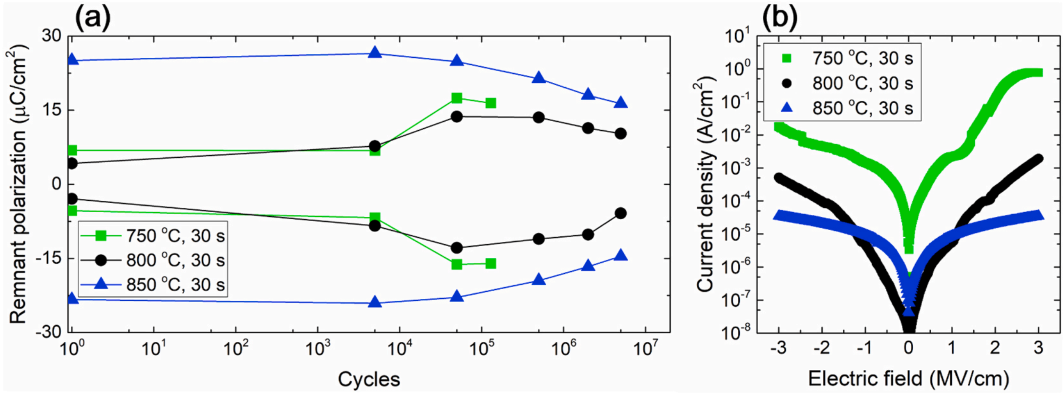

Fig. 5. (a) Endurance characteristics for the capacitors annealed at various annealing temperature under ±4 V bipolar pulses of 5 kHz. The width of the one pulse was 50 μs. (b) The current density of the HZO thin film varied in different annealing temperatures.

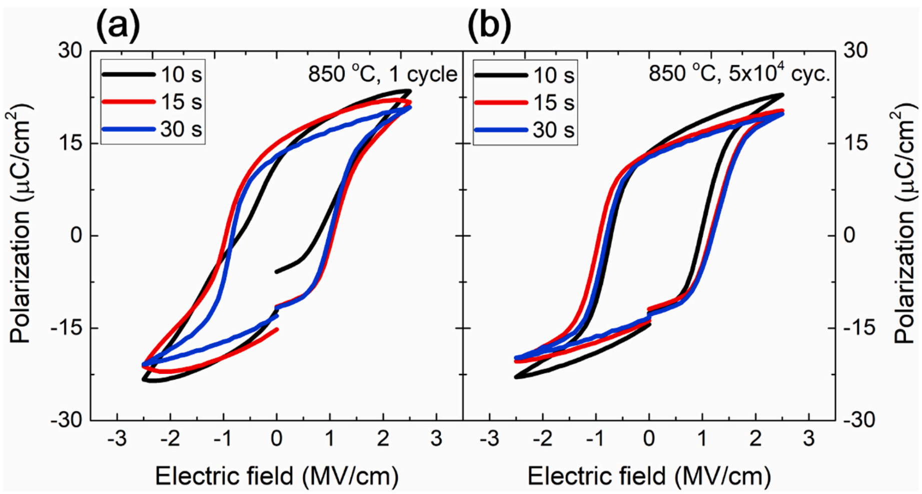

Fig. 6. (a) The initial P-E curves for the capacitors as a function of annealing time. (b) The ferroelectric behaviors were clearly shown after the pulses were applied.

dielectric constant obtained from the C–V measurement, as shown in the inset of Fig. 3b. The overall impact of annealing temperature on the ferroelectric behavior could be also confirmed by tracing current density as a function of time, as shown in Fig. 3c and 3d. The two peaks of the current density due to defects appeared broadly in the pristine state over the entire range of annealing temperatures, except 850 °C (Fig. 3c). The wake-up pulses drove the conversion to open hysteresis, leading to a single merged peak (Fig. 3d).

The achieved ferroelectric properties resulted from the formation of orthorhombic phases, which could be indirectly confirmed by GIXRD analysis. The peak intensity at 2θ of about 30.3 ° indicated orthorhombic, tetragonal, and cubic phases, as shown in both capacitors annealed at 800 and 850 °C, (Fig. 4). In addition to the mixed phase, the GIXRD data exhibited peaks at 2θ of 28 and 34.5 ° representing monoclinic phases. The higher annealing temperature increased the orthorhombic phase by reducing the monoclinic phase. The involvement of more active phases in the switching can thus be the reason why the ferroelectric behaviors were shown in the first cycle of measurement for the capacitor annealed at 850 °C.

In the capacitors annealed by insufficient annealing temperatures of 750 and 800 °C, the phases in the HZO were steadily activated by about 10^5 pulses resulting in a progressively increased P_r, as shown in Fig. 5a. As the interference induced by the leakage was minimized at higher annealing temperature, the ferroelectric operations were maintained under the 5×10^6 cycles without permanent breakdown. Unlike previous cases where the wake-up process was needed, the large P_r continued because the ferroelectric phases were involved in the switching from the beginning.

Fig. 5b shows the current density–electric field curves of the HZO thin films annealed in various temperatures. The higher current density was observed in the HZO layer annealed at 750 °C, which is in good agreement with the leaky P-E curves shown in Fig. 2b. The leakage current was obviously suppressed as the annealing temperature was increased.

Next, annealing time at the given annealing method and annealing temperature was controlled. As evidenced by the annealing temperature dependence, a similar evolution from pinched hysteresis to open hysteresis occurred, as shown in Fig. 6a. After the wake-up process, strong ferroelectric properties with large P_r and rapid transition were achieved no matter what annealing time was applied, as shown in Fig. 6b. These results mean that sufficient annealing temperature and annealing time are necessary to complete the thermodynamic transition.

The switching dynamics of the capacitor was evaluated by measuring the minimum annealing time needed to saturate the degree of change in polarization, as shown in Fig. 7a and b. The capacitor was polarized in a specific direction by negative pulses of 1 ms. A positive pulse of 200 ns was then applied to switch the orientation of the dipoles. This procedure was performed continuously, while increasing just the width of the positive pulse. The magnitude of the saturated polarization varied with the applied voltage amplitude, but most switching behaviors were saturated within 5 μs. The shorter pulse width caused less stress to the capacitor, resulting in reliable fatigue up to 10^8 cycles, as shown in

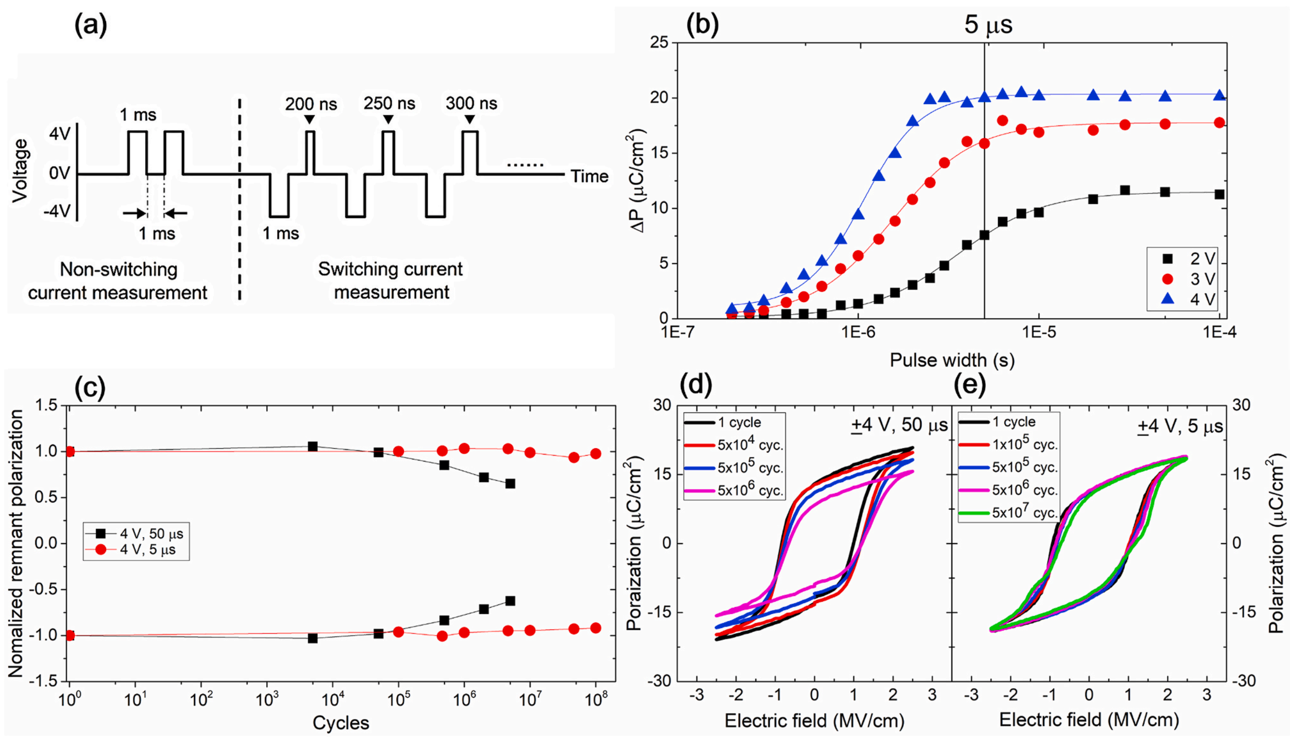

Fig. 7. (a) Schematic diagram of the pulse scheme to extract the minimum pulse width required for the polarization. (b) Time dependent remnant polarization (ΔP) under various pulse amplitudes. (c) More reliable fatigue property was achieved by using short pulse width. Each P–V curve of the capacitors evaluated with pulse width of (d) 50 and (e) 5 μs.

Fig. 7c. The P_r was continuously lowered in each P-E curve with increasing pulses of 50 μs (Fig. 7d), while the stable P_r from the P-E trace was observed with shortened pulse width, as shown in Fig. 7e.

3. Conclusion

In this study, we systematically investigated and demonstrated stable polarization behavior in a sputtered HZO layer, while examining several annealing conditions. Our results showed that the phase transition to the orthorhombic phase seemed to be preferred when the HZO was annealed in the presence of TE. In addition, as the annealing temperature was increased to 850 °C, not only the leakage was suppressed, but the wake-up process, which is essential for the complete conversion from antiferroelectric-like hysteresis to ferroelectric hysteresis, was also negligible. These results indicate that the ferroelectric phases were easily activated from the beginning under conditions where sufficient annealing temperature and annealing time were provided. We then showed reliable fatigue behavior up to 10^8 cycles driven by repeated cycles with a pulse width of 5 μs, which was extracted from the switching dynamics analysis.

Declaration of competing interest

The authors declare that they have no known competing financial interests or personal relationships that could have appeared to influence the work reported in this paper.

Acknowledgements

This work was supported by the National Research Council of Science & Technology (NST) grant by the Korea government (MSIT) (No. CAP-14-01-KIST), the National Research Foundation (NRF) of Korea grant funded by the Korean Government (MSIT) (NRF-2020M3F3A2A01081775), and by the Electronics and Telecommunications Research Institute (ETRI) grant funded by the Korean government (20ZB1100, 20YB1900).

References

[1] J. Müller, T.S. Böscke, S. Müller, E. Yurchuk, P. Polakowski, J. Paul, D. Martin, T. Schenk, K. Khullar, A. Kersch, W. Weinreich, S. Riedel, K. Seidel, A. Kumar, T. M. Arruda, S.V. Kalinin, T. Schlösser, R. Boschke, R. van Bentum, U. Schröder, T. Mikolajick, Ferroelectric Hafnium Oxide: a CMOS-compatible and highly scalable approach to future ferroelectric memories, IEDM (2013) 13–282, https://doi.org/10.1109/IEDM.2013.6724605, 10.8.1-10.8.4.

[2] J. Müller, P. Polakowski, S. Müller, T. Mikolajick, Ferroelectric hafnium oxide based materials and devices: assessment of current status and future prospects, J. Solid State Sci. Technol. 4 (2015) N30–N35, https://doi.org/10.1149/2.0081505jss.

[3] S. Dünkel, M. Trentzsch, R. Richter, P. Moll, C. Fuchs, O. Gehring, M. Majer, S. Wittek, B. Müller, T. Melde, H. Mulaosmanovic, S. Slesazeck, S. Müller, J. Ocker, M. Noack, D.-A. Löhr, P. Polakowski, J. Müller, T. Mikolajick, J. Höntschel, B. Rice, J. Pellerin, S. Beyer, A FeFET based super-low-power ultra-fast embedded NVM technology for 22nm FDSOI and beyond, IEDM (2017) 17–485, https://doi.org/10.1109/IEDM.2017.8268425, 19.7.1-19.7.4.

[4] J. Müller, T.S. Böscke, U. Schröder, S. Müller, D. Brähaus, U. Böttger, L. Frey, T. Mikolajick, Ferroelectricity in simple binary ZrO_2 and HfO_2, Nano Lett. 12 (2012) 4318–4323, https://doi.org/10.1021/nl302049k.

[5] M.H. Park, H.J. Kim, Y.J. Kim, W.K. Lee, H.K. Kim, C.S. Hwang, Effect of forming gas annealing on the ferroelectric properties of $Hf_{0.5}Zr_{0.5}O_2$ thin films with and without Pt electrodes, Appl. Phys. Lett. 102 (2013) 112914, https://doi.org/10.1063/1.4798265.

[6] T.S. Böscke, J. Müller, D. Bräuhaus, U. Schröder, U. Böttger, Ferroelectricity in hafnium oxide thin films, Appl. Phys. Lett. 99 (2011) 102903, https://doi.org/10.1063/1.3634052.

[7] S. Starschich, U. Böttger, An extensive study of the influence of dopants on the ferroelectric properties of HfO_2, J. Mater. Chem. C 5 (2017) 333–338, https://doi.org/10.1039/C6TC04807B.

[8] S. Müller, J. Müller, A. Singh, S. Riedel, J. Sundqvist, U. Schröder, T. Mikolajick, Incipient ferroelectricity in Al-doped HfO_2 thin films, Adv. Funct. Mater. 22 (2012) 2412–2417, https://doi.org/10.1002/adfm.201103119.

[9] J. Müller, U. Schröder, T.S. Böscke, I. Müller, U. Böttger, L. Wilde, J. Sundqvist, M. Lemberger, P. Kücher, T. Mikolajick, L. Frey, Ferroelectricity in yttrium-doped hafnium oxide, J. Appl. Phys. 110 (2011) 114113, https://doi.org/10.1063/1.3667205.

[10] E. Yurchuk, J. Müller, S. Knebel, J. Sundqvist, A.P. Graham, T. Melde, U. Schröder, T. Mikolajick, Impact of Layer Thickness on the Ferroelectric Behaviour of Silicon

Doped Hafnium Oxide Thin Films, vol. 533, 2013, pp. 88–92, https://doi.org/10.1016/j.tsf.2012.11.125.

[11] A. Toriumi, L. Xu, S. Shibayama, S. Migita, Ferroelectric Films by Physical Vapor Deposition and Ion Implantation (Ferroelectricity in Doped Hafnium Oxide: Materials, Properties and Devices), Woodhead Publishing Series in Electronic and Optical Materials, 2019, pp. 103–119, https://doi.org/10.1016/B978-0-08-102430-0.00009-7.

[12] M.H. Park, H.J. Kim, Y.J. Kim, Y.H. Lee, T.H. Moon, K.D. Kim, S.D. Hyun, C. S. Hwang, Study on the size effect in $Hf_{0.5}Zr_{0.5}O_2$ films thinner than 8 nm before and after wake-up field cycling, Appl. Phys. Lett. 107 (2015) 192907, https://doi.org/10.1063/1.4935588.

[13] S.J. Kim, J. Mohan, H.S. Kim, J.B. Lee, C.D. Young, L. Colombo, S.R. Summerfelt, T. San, J.Y. Kim, Low-voltage operation and high endurance of 5-nm ferroelectric $Hf_{0.5}Zr_{0.5}O_2$ capacitors, Appl. Phys. Lett. 113 (2018) 182903, https://doi.org/10.1063/1.5052012.

[14] T. Schenk, E. Yurchuk, S. Müller, U. Schröder, S. Starschich, U. Böttger, T. Mikolajick, About the deformation of ferroelectric hysteresis, Appl. Phys. Rev. 1 (2014), 041103, https://doi.org/10.1063/1.4902396.

[15] H.J. Kim, M.H. Park, Y.J. Kim, Y.H. Lee, T.H. Moon, K.D. Kim, S.D. Hyun, C. S. Hwang, A study on the wake-up effect of ferroelectric $Hf_{0.5}Zr_{0.5}O_2$ films by pulse-switching measurement, Nanoscale 8 (2016) 1383–1389, https://doi.org/10.1039/C5NR05339K.

[16] T. Schenk, U. Schröder, Milan Pešic, mihaela popovici, yuriy V. Pershin, and T. Mikolajick, electric field cycling behavior of ferroelectric hafnium oxide, Appl. Mater. Interfaces 6 (2014) 19744–19751, https://doi.org/10.1021/am504837r.

[17] Milan Pešic, F.P. Gustav Fengler, L. Larcher, A. Padovani, T. Schenk, E.D. Grimley, X. Sang, J.M. LeBeau, S. Slesazeck, U. Schröder, T. Mikolajick, Physical mechanisms behind the field-cycling behavior of HfO_2-based ferroelectric capacitors, Adv. Funct. Mater. 26 (2016) 4601–4612, https://doi.org/10.1002/adfm.201600590.

[18] S. Müller, J. Müller, R. Hoffmann, E. Yurchuk, T. Schlösser, R. Boschke, J. Paul, M. Goldbach, T. Herrmann, A. Zaka, U. Schröder, T. Mikolajick, From MFM capacitors toward ferroelectric transistors: endurance and disturb characteristics of HfO_2-based FeFET devices, IEEE Trans. Electron. Dev. 60 (2013) 4199–4205, https://doi.org/10.1109/TED.2013.2283465.

[19] T. Ali, P. Polakowski, S. Riedel, T. Büttner, T. Kämpfe, M. Rudolph, B. Pätzold, K. Seidel, D. Löhr, R. Hoffmann, M. Czernohorsky, K. Kühnel, P. Steinke, J. Calvo, K. Zimmermann, J. Müller, High endurance ferroelectric hafnium oxide-based FeFET memory without retention penalty, IEEE Trans. Electron. Dev. 65 (2018) 3769–3774, https://doi.org/10.1109/TED.2018.2856818.

[20] Kai Ni, Pankaj Sharma, Jianchi Zhang, Matthew Jerry, Jeffery A. Smith, Kandabara Tapily, Robert Clark, Souvik Mahapatra, Suman Datta, Critical role of interlayer in $Hf_{0.5}Zr_{0.5}O_2$ ferroelectric FET nonvolatile memory performance, IEEE Trans. Electron. Dev. 65 (2018) 2461–2469, https://doi.org/10.1109/TED.2018.2829122.

[21] Wenwu Xiao, Chen Liu, Peng Yue, Shuaizhi Zheng, Feng Qian, Chunfu Zhang, Jincheng Zhang, Hao Yue, Min liao, and yichun zhou, performance improvement of $Hf_{0.5}Zr_{0.5}O_2$-based ferroelectric-field-effect transistors with ZrO_2 seed layers, IEEE Electron. Device Lett. 40 (2019) 714–717, https://doi.org/10.1109/LED.2019.2903641.

[22] K.-T. Chen, H.-Y. Chen, C.-Y. Liao, G.-Y. Siang, C. Lo, M.-H. Liao, K.-S. Li, S. T. Chang, M.H. Lee, Non-volatile ferroelectric FETs using 5-nm $Hf_{0.5}Zr_{0.5}O_2$ with high data retention and read endurance for 1T memory applications, IEEE Electron. Device Lett. 40 (2019) 399–402, https://doi.org/10.1109/LED.2019.2896231.

[23] K.D. Kim, S.D. Hyun, C.S. Hwang, Optimizing process conditions for improved $Hf_{1-x}Zr_xO_2$ ferroelectric capacitor performance, Microelectron. Eng. 178 (2017) 48–51, https://doi.org/10.1016/j.mee.2017.04.031.

[24] S.-J. Yoon, S.-Y. Na, S.E. Moon, S.-M. Yoon, Polarization switching kinetics of the ferroelectric Al-doped HfO_2 thin films prepared by atomic layer deposition with different ozone doses, Vac. Sci. Technol. B 37 (2019), 50601, https://doi.org/10.1116/1.5110621.

[25] S.-N. Chio, S.E. Moon, S.-M. Yoon, Film thickness-dependent ferroelectric polarization switching dynamics of undoped HfO_2 thin films prepared by atomic layer deposition, Ceram. Int. 45 (2019) 22642–22648, https://doi.org/10.1016/j.ceramint.2019.07.297.

[26] T.H. Ryu, S.-Y. Na, S.-M. Yoon, Crystallization annealing effects on ferroelectric properties of Al-Doped HfO_2 thin film capacitors using indium–tin–oxide electrodes, Curr. Appl. Phys. 19 (2019) 1383–1390, https://doi.org/10.1016/j.cap.2019.09.003.

[27] S.-Y. Na, S.-J. Yoon, S.E. Moon, S.-M. Yoon, Characterization of metal–ferroelectric–metal–insulator–semiconductor structures using ferroelectric Al-doped HfO2 thin films prepared by atomic-layer deposition with different O_3 doses, Jpn. J. Appl. Phys. 58 (2019), 070907, https://doi.org/10.7567/1347-4065/ab2c62.

[28] T. Olsen, U. Schröder, S. Müller, A. Krause, D. Martin, A. Singh, J. Müller, M. Geidel, T. Mikolajick, Co-sputtering yttrium into hafnium oxide thin films to produce ferroelectric properties, Appl, Phys. Lett. 101 (2012), 82905, https://doi.org/10.1063/1.4747209.

[29] Y.H. Lee, H.J. Kim, T.H. Moon, K.D. Kim, S.D. Hyun, H.W. Park, Y.B. Lee, M. H. Park, C.S. Hwang, Preparation and characterization of ferroelectric $Hf_{0.5}Zr_{0.5}O_2$ thin films grown by reactive sputtering, Nanotechnology 28 (2017) 305703, https://doi.org/10.1088/1361-6528/aa7624.

[30] Z. Fan, J. Xiao, J. Wang, L. Zhang, J. Deng, Z. Liu, Z. Dong, J. Wang, J. Chen, Ferroelectricity and ferroelectric resistive switching in sputtered $Hf_{0.5}Zr_{0.5}O_2$ thin films, Appl. Phys. Lett. 108 (2016) 232905, https://doi.org/10.1063/1.4953461.

[31] Qing Luo, Hailei Su, Kan-Hao Xue, Rongrong Cao, Zhaomeng Gao, Jie Yu, Tiancheng Gong, Xiaoxin Xu, Jiahao Yin, Yuan Peng, Tai Lu, Danian Dong, Shibing Long, Liu Qi, Xiang-Shui Miao, Hangbing Lv, Ming Liu, Composition-dependent ferroelectric properties in sputtered $Hf_XZr_{1-X}O_2$ thin films, IEEE Electron. Device Lett. 40 (2019) 570–573, https://doi.org/10.1109/LED.2019.2902609.

[32] Chien Liu, Yi-Chun Tung, Chih-Yang Tseng, Wei-Chun Wang, Hsuan-Han Chen, Tsung-Ming Lee, Wu-Ching Chou, Zhi-Wei Zheng, Chun-Hu Cheng, Hsiao-Hsuan Hsu, Stabilizing ferroelectric domain switching of hafnium aluminum oxide using metal nitride electrode engineering, ECS J. Solid State Sci. Technol 8 (2019) 553–556, https://doi.org/10.1149/2.0041910jss.

[33] J. Woo, Y. Goh, S. Im, J.H. Hwang, Y. kim, J.H. Kim, J.-P. Im, S.-M. Yoon, S. E. Moon, S.J. Jeon, Improved ferroelectric switching in sputtered $HfZrO_x$ device enabled by high pressure annealing, IEEE Electron. Device Lett. 41 (2020) 232–235, https://doi.org/10.1109/LED.2019.2959802.

[34] D.-H. Min, S.E. Moon, S.-M. Yoon, Design strategies for improvement in nonvolatile memory characteristics of metal-ferroelectric-metal-insulator semiconductor capacitors using ferroelectric $Hf_{0.5}Zr_{0.5}O_2$ thin films, J. Phys. D Appl. Phys. 40 (2019) 115109, https://doi.org/10.1088/1361-6463/ab622d.

[35] A. Chernikova, M. Kozodaev, A. Markeev, Y. Matveev, D. Negrov, O. Orlov, Confinement-free annealing induced ferroelectricity in $Hf_{0.5}Zr_{0.5}O_2$ thin films, Microelectron. Eng. 147 (2015) 15–18, https://doi.org/10.1016/j.mee.2015.04.024.

[36] R. Cao, Y. Wang, S. Zhao, Y. Yang, X. Zhao, W. Wang, X. Zhang, H. Lv, Q. Liu, M. Liu, Effects of capping electrode on ferroelectric properties of $Hf_{0.5}Zr_{0.5}O_2$ thin films, IEEE Electron. Device Lett. 39 (2018) 1207–1210, https://doi.org/10.1109/LED.2018.2846570.

[37] Y.-.C. Lin, F. McGuire, A.D. Franklin, Realizing ferroelectric $Hf_{0.5}Zr_{0.5}O_2$ with elemental capping layers, J. Vac. Sci. Technol. B 36 (2018), 11204, https://doi.org/10.1116/1.5002558.